

SG-Splatting: Accelerating 3D Gaussian Splatting with Spherical Gaussians

Yiwen Wang¹, Siyuan Chen¹, Ran Yi¹

¹Shanghai Jiao Tong University
wangyiwewn999@sjtu.edu.cn, gouliguojiashengsiyi@sjtu.edu.cn, ranyi@sjtu.edu.cn

Abstract

3D Gaussian Splatting is emerging as a state-of-the-art technique in novel view synthesis, recognized for its impressive balance between visual quality, speed, and rendering efficiency. However, reliance on third-degree spherical harmonics for color representation introduces significant storage demands and computational overhead, resulting in a large memory footprint and slower rendering speed. We introduce SG-Splatting with Spherical Gaussians based color representation, a novel approach to enhance rendering speed and quality in novel view synthesis. Our method first represents view-dependent color using Spherical Gaussians, instead of three degree spherical harmonics, which largely reduces the number of parameters used for color representation, and significantly accelerates the rendering process. We then develop an efficient strategy for organizing multiple Spherical Gaussians, optimizing their arrangement to achieve a balanced and accurate scene representation. To further improve rendering quality, we propose a mixed representation that combines Spherical Gaussians with low-degree spherical harmonics, capturing both high- and low-frequency color information effectively. SG-Splatting also has plug-and-play capability, allowing it to be easily integrated into existing systems. This approach improves computational efficiency and overall visual fidelity, making it a practical solution for real-time applications.

Introduction

Novel view synthesis is an important task in computer graphics and vision, focusing on generating new perspectives of a scene from a limited set of multi-view images. This task addresses the challenge of creating realistic and immersive novel view images without requiring extensive data collection or manual modeling. The advent of 3D Gaussian Splatting (Kerbl et al. 2023) has injected new momentum into the field of novel view synthesis. Before the introduction of 3D Gaussian Splatting, NeRF (Mildenhall et al. 2020) models, which rely on MLP for novel view synthesis, were widely used but suffered from slow inference times and lengthy training processes. In contrast, 3D Gaussian Splatting leverages Gaussian splats to represent scene geometry and appearance, offering significant improvements in rendering speed, image quality, and training efficiency. This approach effectively addresses the limitations of NeRF, providing a more practical and scalable solution for applica-

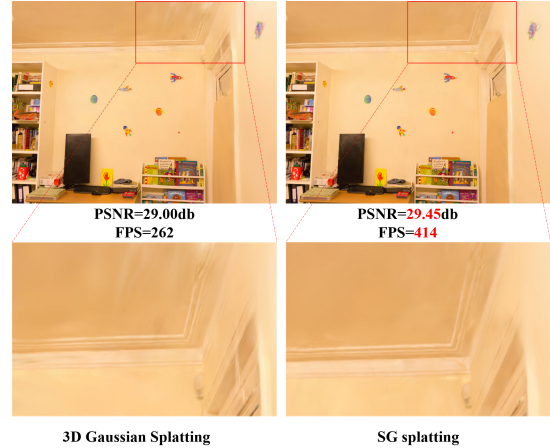


Figure 1: **SG-Splatting: Spherical Gaussian-Based Splatting.** The top row presents comparisons of SG-Splatting and 3D-GS on rendering results and quantitative metrics on the DeepBlending (Hedman et al. 2018) dataset, demonstrating the ability to achieve rapid rendering. The bottom row provides zoom-in qualitative analysis of the rendered scenes, highlighting how 3D-GS exhibits noticeable artifacts, which are effectively minimized by our SG-Splatting approach.

tions requiring fast and high-quality view generation, such as virtual reality (Jiang et al. 2024), 3D&4D content generation (Shao et al. 2024; Yang et al. 2024), physical simulation (Xie et al. 2023; Zhong et al. 2024) and autonomous driving (Zhou et al. 2024).

Despite its advancements, 3D Gaussian Splatting faces significant challenges that limit its broader application, particularly in real-time rendering environments. One of the primary limitations is its reliance on third-degree spherical harmonics (SH) for color representation. While this approach allows for detailed and accurate color expression, it comes at the cost of a substantial memory footprint: each Gaussian requires 48 SH coefficients, considering a scene with millions of Gaussians, the total number of SH coefficients is huge. The high storage requirements not only consume a large amount of computational resources, but also restrict the scalability of the technique in more complex or larger scenes. Additionally, the use of spherical harmonics introduces computational complexity that impacts the rendering

speed. The forward inference process requires considerable calculations, leading to slower rendering times, which can be a critical bottleneck in applications demanding real-time performance.

To address the challenges posed by the large memory footprint and slow rendering speed of 3D Gaussian Splatting, several recent studies, including LightGaussian (Fan et al. 2023) and Compact3D (Navaneet et al. 2023), have focused on compressing the model size of 3D Gaussian Splatting to make it more efficient. These approaches primarily leverage traditional model compression techniques, such as knowledge distillation (Hinton, Vinyals, and Dean 2015) and vector quantization (Jacob et al. 2018), to reduce the size of the model while attempting to maintain its visual quality. While these methods have shown promise in reducing the computational demands of 3D Gaussian Splatting, they overlooked the potential optimizations within the 3D Gaussian Splatting representation itself, which could lead to significant space compression and rendering acceleration.

Upon further investigation, we identified that the most significant parameter overhead in 3D Gaussian Splatting stems from the coefficients of the spherical harmonics used for color representation. Specifically, the use of third-degree spherical harmonics results in more than half of the model’s parameters being allocated to storing these coefficients¹, contributing to the substantial memory requirements and computational burden. To address this issue, we propose **SG-Splatting** with novel **Spherical Gaussians based color representation**, which offers a more compact and efficient representation. Firstly, we propose to represent view-dependent color using Spherical Gaussians, instead of three-degree SH, largely reducing the number of parameters required for color representation. Secondly, we propose the use of multiple Spherical Gaussians of orthogonal orientations, to better simulate and optimize the scene, achieving a balance between reduced parameter overhead and enhanced rendering performance. Furthermore, we propose a mixed color representation that combines Spherical Gaussians with adaptive low-degree spherical harmonics, which combines the advantages of SG in high-frequency color representation, and the advantages of low-degree SH in low-frequency color representation, to further improve rendering quality. This approach accelerates the rendering process, making it more suitable for real-time applications.

Contributions of this paper can be summarized as:

- **Spherical Gaussians based Color Representation:** We propose SG-Splatting, an innovative approach that represents view-dependent color using Spherical Gaussians, instead of three-degree spherical harmonics, significantly reducing the model’s parameter overhead and improving computational efficiency.
- **Effective Organization of Multiple Spherical Gaussians:** To further enhance the model’s performance, we develop a method for the effective organization of multiple spherical Gaussians, optimizing scene representation while maintaining high visual fidelity.

¹In 3D-GS, each Gaussian has 59 parameters for geometry and texture representation, where 48 parameters are SH coefficients.

- **Mixed Spherical Gaussians and low-degree spherical harmonics representation:** We further propose a mixed color representation that combines the advantages of Spherical Gaussians in representing high-frequency color and the advantages of low-degree spherical harmonics in representing low-frequency color, to enhance rendering quality.
- **Plug-and-Play Capability:** Our experiments show that SG-Splatting can be seamlessly integrated into other acceleration methods. This plug-and-play capability allows our approach to enhance existing techniques, improving rendering speed while maintaining output quality.

Related Works

Novel View Synthesis

Novel view synthesis (NVS) traditionally relies on Structure-from-Motion (SfM) (Schönberger and Frahm 2016) and Multi-View Stereo (MVS) (Schönberger et al. 2016), where SfM reconstructs a scene’s 3D structure from multiple images, providing the initial geometry for further processing.

Neural Radiance Fields (NeRF) (Mildenhall et al. 2020) brought a significant advancement to NVS by using a multi-layer perceptron (MLP) for volumetric scene modeling, though it suffers from slow training and rendering. Subsequent methods like Mip-NeRF 360 (Barron et al. 2022) improved image quality but at the cost of higher computational demands, while InstantNGP (Müller et al. 2022) and PlenOctree (Yu et al. 2021) focused on speeding up training and rendering, respectively.

Recently, 3D Gaussian Splatting (3D-GS) has emerged as a more efficient alternative for NVS, surpassing NeRF in both speed and quality. By approximating radiance fields with Gaussian components, 3D-GS enables real-time rendering, making it a transformative development for novel view synthesis.

3D-GS Fast Inference

As an explicit rendering method, the inference speed of 3D Gaussian Splatting is closely related to the number of Gaussians used. The inference process cost ϵ of 3D Gaussian Splatting can be approximately quantified as:

$$\epsilon = N \times C, \quad (1)$$

where N represents the total number of Gaussians in the system, and C denotes the computational cost associated with processing each individual Gaussian. This relationship highlights the direct impact of the number of Gaussians on the overall computational expense, emphasizing the importance of efficient representation and processing within the 3D Gaussian Splatting framework.

To accelerate inference process, GES (Hamdi et al. 2024) reduces the number of Gaussians by optimizing Gaussian expressions using generalized exponential functions. LightGaussian (Fan et al. 2023) trims Gaussians based on their importance, determined by factors like opacity and volume. Compact3D (Navaneet et al. 2023) employs a learnable mask to prune Gaussians effectively. Mini-splatting (Fang

and Wang 2024) decreases sampling points by incorporating depth estimation, While Eagles (Girish, Gupta, and Shrivastava 2023) and Compress3D (Niedermayr, Stumpfegger, and Westermann 2023) use quantized methods to compress attributes like color and direction of Gaussian primitives. Although these methods have achieved notable success in speeding up the rendering process, they have not directly modified the most impactful component in Gaussian representation, the spherical harmonics (SH).

Color Representation

In novel view synthesis and computer graphics, color representation is crucial. Methods like NeRF use end-to-end MLPs to learn color information, but this approach demands significant computational resources, leading to long rendering times. To mitigate these challenges, SNeRG (Hedman et al. 2021) separated appearance into diffuse and specular components, reducing reliance on large MLPs and cutting down on inference time. Building on this, PlenOctree (Yu et al. 2021) introduced spherical harmonics (SH) for color representation, effectively approximating spherical fitting and improving efficiency for scenes viewed from various angles.

Other techniques, such as spherical functions (Wang et al. 2009; Xu et al. 2013) and wavelet transforms (Ng, Ramamoorthi, and Hanrahan 2003), have also been explored for color representation and storage. These methods efficiently capture and compress color information while preserving detail, enabling faster rendering and reduced storage requirements.

In comparison, Spherical Gaussians (SG) are the most flexible and computationally lightweight option. With fewer parameters and simpler computations, SGs are ideal for accelerating rendering while maintaining high quality, making them well-suited for novel view synthesis.

Methods

Overview

The original 3D Gaussian Splatting system, due to its reliance on three degree spherical harmonics, requires a large number of parameters to store the spherical harmonic coefficients. This results in a significant increase in the model’s memory usage and also adversely affects the forward rendering speed. We propose SG-Splatting, a novel 3D Gaussian Splatting technique designed to overcome the limitations of traditional spherical harmonics by using **Spherical Gaussians (SG) based color representation**.

As shown in Fig. 2, our SG-Splatting framework builds upon 3D-GS by incorporating Spherical Gaussians to form a more compact color representation. The inputs and output of our system are the same as original 3D-GS: The inputs consists of multi-view scene images and their corresponding camera parameters, and the output is the final rendered image of the scene. The process begins by using the multi-view images to generate an initial point cloud by SfM. This point cloud is then used to initialize elliptical Gaussians, which represent the scene’s geometry and color, where the color

adopts our SG-based representation. These elliptical Gaussians are optimized by minimizing the loss between the rendered image and the ground truth, using alpha blending to produce the final scene renderings.

Different from original 3D-GS that uses three degree spherical harmonics (SH) for color representation, to enhance rendering quality while maintaining efficiency, we further propose a **mixed color representation that combines Spherical Gaussians and adaptive low-degree spherical harmonics**. 1) The *high-frequency color component* is represented using Spherical Gaussians, which is more compact than SH, and excels at representing high-frequency color components, to capture fine lighting and shading details. Using single SG requires only 7 parameters to represent view-dependent color, much fewer than 45 parameters required by three-degree SH. Furthermore, we propose to use multiple SGs of orthogonal orientations to complement each other and improve the modeling of color and light. This orthogonal arrangement ensures that each Gaussian can effectively represent distinct aspects of the scene’s color and light, minimizing redundancy and improving the overall rendering quality. 2) Meanwhile, the *low-frequency color component* is initially expressed using a simple 3-dimensional diffuse color (the zero degree SH component), with the option to replace this with adaptive low-degree SH (0-2 degree) for a better balance between rendering speed and quality. Although using low-degree SH alongside Spherical Gaussians may slightly reduce rendering speed, it significantly improves the overall rendering quality, making this trade-off beneficial for scenarios where visual fidelity is a priority.

Preliminaries

3D Gaussian Splatting (3D-GS) is an explicit method for modeling scenes in novel view synthesis using a set of 3D Gaussian ellipsoids with geometric and texture properties.

The geometry of each Gaussian is parameterized by its center position X and a covariance matrix Σ . The covariance matrix defines the shape, size, and orientation of the Gaussian, allowing it to model the spatial distribution of the data. Therefore, given a point x in the 3D space, the Gaussian function is defined as:

$$G(x) = e^{-\frac{1}{2}(x-\mathbf{X})^T \Sigma^{-1}(x-\mathbf{X})}, \quad (2)$$

where the covariance matrix is typically decomposed into a rotation matrix R (represented by a quaternion q) and a scaling matrix S (represented by a scaling vector s). This decomposition ensures that the Gaussian primitives are appropriately oriented and scaled in the 3D space:

$$\Sigma = R S S^T R^T. \quad (3)$$

The texture information of each Gaussian consists of opacity σ and spherical harmonics (to represent color). For rendering, the 3D Gaussian primitives are first projected into 2D space from a given viewpoint (Zwicker et al. 2002). Once projected, the overlapping splats are accumulated and blended to create the final image.

Spherical Harmonics (SH). To achieve high-quality rendering, particularly in capturing complex lighting and shad-

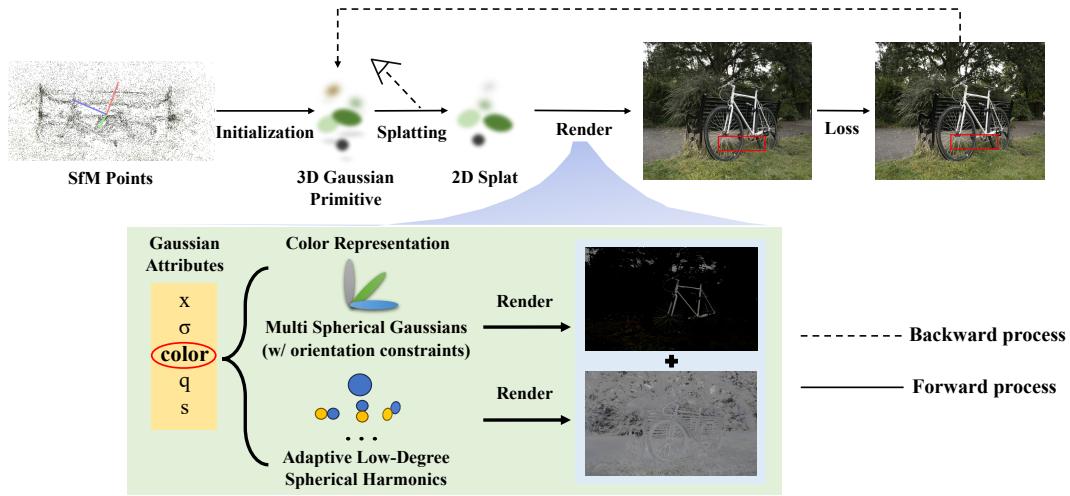


Figure 2: Our SG-Splatting framework for novel view synthesis. The process begins with multi-view images and corresponding camera views, which are used to initialize Gaussian primitives through SfM. These primitives are characterized by their positions, covariance matrices, opacity and color information. High-frequency color components are represented using Spherical Gaussians (SGs) to accurately capture view-dependent effects, while low-frequency color components are supplemented using diffuse or adaptive low-degree Spherical Harmonics (SH) to provide a smooth and consistent representation. The final rendered output is compared with the ground truth to evaluate the method performance.

ing effects, 3D-GS utilizes three degree spherical harmonics (SH) to represent the scene’s color. Spherical harmonics have components that carry specific physical meanings, stemming from their mathematical origins in solving the angular part of Laplace’s equation in spherical coordinates. These components are particularly useful in representing angular functions and capturing the directional properties of light and sound in various physical systems. Specifically, 3D-GS uses the following formula to represent color by SH:

$$c(\mathbf{v}) = \sum_{l=0}^L \sum_{m=-l}^l c_{lm} Y_{lm}(\mathbf{v}), \quad (4)$$

where \mathbf{v} is the input viewing direction, $c(\mathbf{v})$ is the color observed from that direction, c_{lm} is the spherical harmonic coefficient, and $Y_{lm}(\mathbf{v})$ is the spherical harmonic basis function of degree l and order m . The sum is taken over all degrees l and orders m up to a specified level $L = 3$, capturing the complexity of the color variations.

Each SH has a fixed and distinct shape. For a given spherical function, these SHs need to be combined and their coefficients adjusted to accurately fit the function. This process involves fine-tuning each coefficient to capture the specific features and details of the spherical function being represented. However, for three degree SH, the entire 3D-GS system requires 16 SH coefficients for each color channel, and 48 SH coefficients in total. This results in a significant increase in the model’s parameter count, contributing to the substantial memory overhead and computational complexity associated with the system.

Spherical Gaussian based Color Representation

To address the inefficiencies associated with spherical harmonics, *i.e.*, requiring 48 SH coefficients for color represen-

tation, we propose to use Spherical Gaussians for color representation. Spherical Gaussians are more lightweight and flexible than spherical harmonics, primarily because they require fewer parameters (10 compared to 48 of SH) and can be easily adjusted to point in specific orientations.

Background on Spherical Gaussians (SG). As shown in Figure 3, the geometric shape of Spherical Gaussians resembles lobes, allowing for more precise control of light and color representation in different directions. Different from spherical harmonics (SH) that have fixed shapes and cannot be adjusted in form or position, Spherical Gaussians (SG) offer flexibility in that: the orientation of lobe can be arbitrarily adjusted by parameter μ , and the sharpness of lobe can be controlled by parameter λ (see visualizations of different μ and λ in Figure 3). This ability to dynamically adjust both orientation and sharpness gives Spherical Gaussians a distinct advantage in rendering applications, allowing for more accurate and versatile representations.

SG-based Color Representation. Based on Spherical Gaussians, the color C of each Gaussian is represented as:

$$C(d; \alpha, \lambda, \mu) = \alpha e^{\lambda(d \cdot \mu - 1)}, \quad (5)$$

where d is the direction of the view, λ controls the sharpness of the lobe, α represents the coefficients for the three color channels, and μ denotes the orientation of the lobe’s peak. A larger value of λ results in a more concentrated lobe, increasing the sharpness of the effect.

To further enhance the accuracy of color representation, we decompose the color into two components: diffuse, and view-dependent. The diffuse component captures the inherent color of the surface that is independent of the viewing angle; while the view-dependent component captures effects such as specular highlights, which vary depending on the

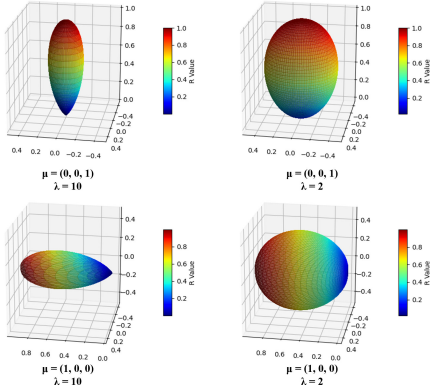


Figure 3: Visualization of Spherical Gaussians (SG) and how variations in μ and λ affect the orientation and sharpness of SG. Comparing the top and bottom row highlights the differences in μ , which changes the orientation of the SG. Comparing from left to right illustrates the effect of sharpness λ ; as λ increases, the SG becomes more concentrated, resulting in a sharper peak.

viewer’s position relative to the light source. Therefore, the color is represented as:

$$C(d; \alpha, \lambda, \mu) = D + \alpha e^{\lambda(d \cdot \mu - 1)}, \quad (6)$$

where diffuse component D , and coefficients of each color channel α are 3-dimensional vectors, orientation of Spherical Gaussian lobe’s peak μ is also 3-dimensional, and sharpness of Spherical Gaussian lobe λ is a scalar. Therefore, under SG-based representation, each Gaussian requires only 10 parameters (3 for diffuse, 7 for SG) to represent color. This is significantly fewer than the number of parameters (48) needed for each Gaussian under three degree SH-based color representation. This reduction in parameter count highlights the efficiency of Spherical Gaussians, making them a much more compact and computationally efficient alternative, and allows for faster rendering and training speeds.

Multi-Axis Orthogonal Gaussians

While a single Spherical Gaussian significantly enhances rendering speed, it can face challenges in handling complex lighting scenarios, which may result in some limitations in rendering quality. To address this issue, we employ multiple Spherical Gaussians to improve the modeling of color and light, where multiple Spherical Gaussians have different orientations and complement each other.

However, simply accumulating multiple Spherical Gaussians led to suboptimal results (Fig. 4 third column). The primary issue was that the Gaussians failed to distribute the scene’s content effectively, resulting in clustering that further degraded the rendering quality. Spherical Gaussians can have arbitrary orientations of lobe (defined by μ), which make them more flexible, but more difficult to control and combine. *E.g.*, in some scenes, without constraints on orientations of lobe, multiple Spherical Gaussians may be influenced by strong specular highlights in a certain orientation,

and be optimized to similar orientations, failing to achieve the goal of complementarity.

Multiple Orthogonal SGs. To address this limitation, we introduce multiple orthogonal Spherical Gaussians, where the orientations (μ) of multiple Gaussians are orthogonal to each other. This orthogonal arrangement allows different Spherical Gaussians to complement one another more effectively, ensuring better alignment and coherence in the representation. As a result, this approach enhances rendering quality by maintaining a more structured and comprehensive depiction of the scene’s color and light (Fig. 4 fourth column).

Each orthogonal direction acts as a basis vector. By using these orthogonal directions, we achieve a more structured representation of the scene’s color and light, reducing the likelihood of clustering and ultimately leading to improved rendering results. Specifically, the color C is represented as:

$$C(d; \alpha, \lambda) = D + \sum_{i=1}^3 \alpha_i e^{\lambda_i(d \cdot \mu_i - 1)}, \quad (7)$$

$$\mu_i \cdot \mu_j = \begin{cases} 1, & \text{if } i = j, \\ 0, & \text{if } i \neq j. \end{cases} \quad (8)$$

Although introducing multiple Spherical Gaussians increases the number of parameters, this increase is minimized by using orthogonal axes. Each Spherical Gaussian aligned along orthogonal axes requires 4 parameters—coefficients for color α and sharpness λ . Additionally, 3 extra parameters are needed to define the orthogonal directions μ , resulting in a total of 15 parameters for 3 orthogonal SGs. This is still far fewer than the 48 parameters needed for third-degree spherical harmonics. This approach ensures that the multiple SGs complement each other effectively, optimizing the overall representation while keeping the increase in complexity minimal. Moreover, our experiments show that the specific directions of the orthogonal axes are not crucial; the key is maintaining their orthogonality, which simplifies implementation (see Supplementary material for experimental details).

Mixing Spherical Harmonics and Spherical Gaussians

While the use of multiple Spherical Gaussians significantly accelerates the 3D Gaussian Splatting process, it can lead to some loss in rendering quality due to compressed color parameters. To address this and further enhance the rendering quality, we incorporate adaptive low-degree spherical harmonics (0-2 degree) along with Spherical Gaussians for color representation.

Specifically, we adaptively adjust the degree used for SH based on the size of Gaussians. According to statistics on Gaussian radius (detailed in Supplementary material), we observed that most Gaussians in the scene are small. For small Gaussians, their coverage area is limited, and they do not exhibit significant view-dependent changes, mainly containing low-frequency color information. As a result, there is no need to use high-degree spherical harmonics (SH) to fit them, and lower-degree SH is sufficient to capture their characteristics effectively. For these smaller Gaussians, we

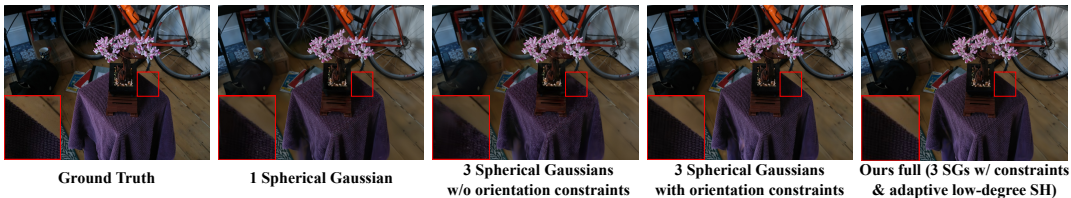


Figure 4: Comparison of rendering results using different numbers of Spherical Gaussians (SGs). Using 3 SGs without orientation constraints can lead to inaccuracies (*e.g.*, incorrectly brightening shadowed areas), while with orthogonal orientation constraints, the rendering quality is improved. Ours full further integrates adaptive low-degree SH for better rendering quality.

calculate their size based on the matrix of their 2D projection, and dynamically choose to use 0th, 1st, or 2nd degree spherical harmonics according to their sizes. While for large Gaussians that are of a small proportion, we use 2nd degree spherical harmonics. This adaptive approach allows us to achieve a balance between rendering speed and quality, ensuring that each Gaussian is represented with the appropriate level of detail:

$$C(d; \alpha, \lambda) = SH + \alpha e^{\lambda(d-\mu-1)}. \quad (9)$$

Experiments

Experiment Settings

Datasets and Metrics. We conduct our experiments on three commonly used datasets: Mip-NeRF360 (Barron et al. 2022), Tanks&Temples (Knapitsch et al. 2017), and DeepBlending (Hedman et al. 2018).

To evaluate SG-Splatting, we use several metrics. Quality is measured using PSNR, SSIM (Wang et al. 2004), and LPIPS (Zhang et al. 2018), which assess image fidelity, structural similarity, and perceptual quality, respectively. Rendering speed is measured in FPS, indicating the method’s efficiency in real-time applications. We also report training time to measure computational efficiency.

All experiments are conducted on an NVIDIA RTX 3090 GPU to ensure fairness and avoid performance variations due to hardware differences.

Implementation. The learning rate hyperparameters for training are consistent with those used in 3D-GS to ensure fair comparison. The total number of training iterations is set to 30,000. After the initial 2,000 iterations, Spherical Gaussians are introduced into the training process with a learning rate of 0.0025. This staged introduction helps in gradually refining the model’s ability to capture complex lighting and shading effects, leading to improved rendering quality. For multiple orthogonal SGs, in our experiments, based on observations that the specific directions of orthogonal axes are not crucial while the key is the orthogonality (see experiments in Supplementary material), we selected the orthogonal axes as $(1, 0, 0)$, $(0, 1, 0)$, and $(0, 0, 1)$ for ease of implementation.

Comparisons

Baselines. We compare SG-Splatting with two groups of baseline methods. 1) The first group includes original 3D-GS, Compact3D (Navaneet et al. 2023) and Eagles (Girish,

Gupta, and Shrivastava 2023), which primarily focus on post-processing trained models through model compression techniques to reduce the number of Gaussian primitives and improve efficiency. 2) The second group, including Mini-splatting (Fang and Wang 2024) and GES (Hamdi et al. 2024), optimizes the 3D-GS model and training process to enhance rendering quality and speed. Our SG-Splatting can be seamlessly integrated into these approaches, offering additional improvements in efficiency.

Results and Analysis

Table 1 presents a comprehensive comparison, including the performance of our SG-Splatting, and the effects of integrating SG-Splatting into other existing approaches. Fig. 5 shows the qualitative comparison results. In comparison with the first group of baselines, our method achieves the fastest rendering speed, 1.4 \sim 1.5 times faster than original 3D-GS; with rendering quality slightly lower than the original 3D-GS, but consistently outperforming other compression-based post-processing methods, particularly in the most complex scenes from Mip-NeRF360. In the second group of baselines, after integrating our SG-based color representation into these methods (Mini-splatting and GES), we observe a significant improvement in rendering speed across most scenes, with only a minor reduction in rendering quality. This demonstrates the effectiveness of our approach in improving efficiency while maintaining high visual fidelity.

Furthermore, SG-Splatting demonstrates a storage size reduction of approximately 46.7% \sim 47.3% between datasets compared to 3D Gaussian Splatting, further enhancing its practicality for memory-constrained environments.

Ablation Studies

We conducted ablation studies by progressively adding our components to the base 3D-GS model to evaluate their impact (Table 2 and Fig. 4). Specifically, we tested the effects on rendering speed, rendering quality, and model size, evaluating how each component contributes to overall performance.

3DGS + Multi-Axis Orthogonal SG: Introducing orthogonal SGs achieves a significant improvement in rendering speed and model size, at the cost of a slight decrease in rendering quality. Specifically, the rendering speed increases from 247 to 371 FPS, while the model size is reduced from 781.46 to 364.01 MB. Although there is a minor drop in PSNR (from 27.410 to 26.845) and SSIM (from 0.814 to 0.803), the trade-off results in a much more efficient model.

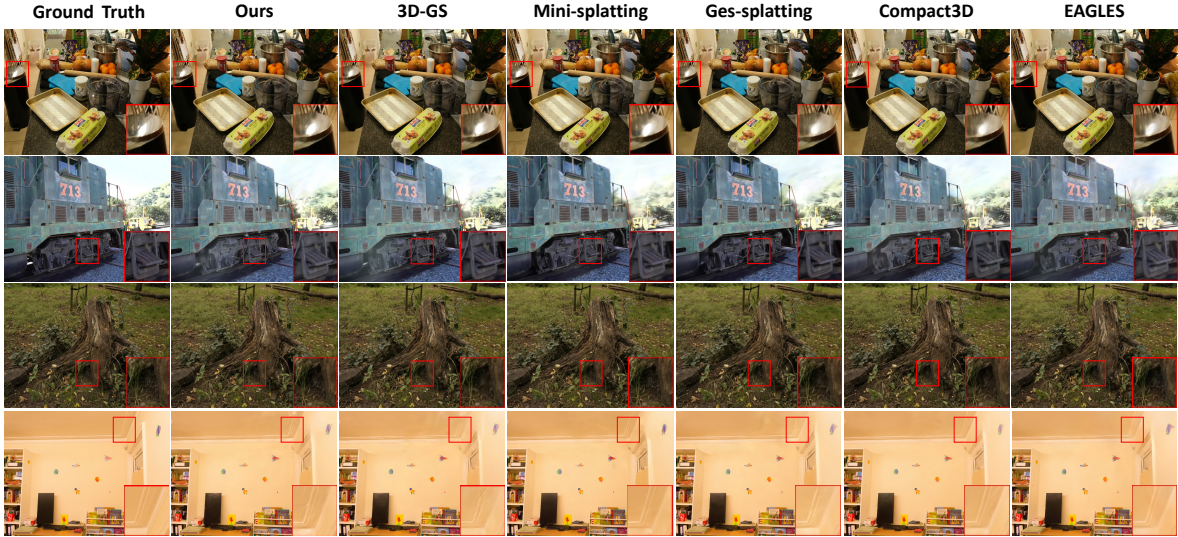


Figure 5: Qualitative comparison of our SG-Splatting with baseline methods.

| Dataset Matrices | Mip-NeRF360 | | | | | Tanks&Temples | | | | | DeepBlending | | | | |
|---------------------|-----------------|-----------------|--------------------|----------------|--------------------|-----------------|-----------------|--------------------|----------------|--------------------|-----------------|-----------------|--------------------|----------------|--------------------|
| | PSNR \uparrow | SSIM \uparrow | LPIPS \downarrow | FPS \uparrow | Train \downarrow | PSNR \uparrow | SSIM \uparrow | LPIPS \downarrow | FPS \uparrow | Train \downarrow | PSNR \uparrow | SSIM \uparrow | LPIPS \downarrow | FPS \uparrow | Train \downarrow |
| 3D-GS | 27.401 | 0.814 | 0.217 | 247 | 25min29s | 23.728 | 0.845 | 0.179 | 312 | 14min40s | 29.508 | 0.900 | 0.247 | 233 | 24min18s |
| Compact3D | 26.969 | 0.797 | 0.245 | 293 | 35min41s | 23.323 | 0.831 | 0.202 | 383 | 20min41s | 29.749 | 0.901 | 0.259 | 331 | 19min50s |
| EAGLES | 27.140 | 0.805 | 0.239 | 155 | 21min55s | 23.342 | 0.836 | 0.200 | 245 | 11min22s | 29.951 | 0.907 | 0.249 | 156 | 19min41s |
| SG-Splatting | 27.267 | 0.813 | 0.218 | 334 | 24min11s | 23.465 | 0.840 | 0.188 | 472 | 13min21s | 29.570 | 0.901 | 0.247 | 344 | 22min25s |
| Mini-splatting | 27.345 | 0.822 | 0.217 | 576 | 21min17s | 23.259 | 0.836 | 0.202 | 685 | 14min12s | 29.962 | 0.908 | 0.248 | 656 | 18min15s |
| SG-mini-Splatting | 26.933 | 0.835 | 0.222 | 681 | 21min05s | 23.036 | 0.833 | 0.205 | 861 | 12min37s | 29.916 | 0.908 | 0.253 | 773 | 17min40s |
| GES | 26.901 | 0.794 | 0.252 | 421 | 20min14s | 23.414 | 0.837 | 0.198 | 518 | 11min02s | 29.628 | 0.901 | 0.252 | 398 | 19min04s |
| SG-GES | 26.703 | 0.791 | 0.260 | 520 | 17min58s | 23.234 | 0.832 | 0.202 | 626 | 10min01s | 29.704 | 0.902 | 0.251 | 488 | 17min37s |

Table 1: Detailed comparison of our SG-Splatting with 3D-GS and other baseline methods across various datasets. In comparison with the first group of baselines, we achieve the fastest rendering speed; and in the second group of baselines, after integrating our SG-Splatting into Mini-splatting and GES, the rendering speed is further improved, showing that our approach enhances efficiency while maintaining high visual quality. The best and second best scores in each group are highlighted in yellow and pink.

| Ablation Setup | PSNR \uparrow | SSIM \uparrow | LPIPS \downarrow | FPS \uparrow | Size(MB) \downarrow |
|---|-----------------|-----------------|--------------------|----------------|-----------------------|
| 3D Gaussian Splatting | 27.410 | 0.814 | 0.217 | 247 | 781.46 |
| 3DGS + Multi-Axis Orthogonal SG | 26.845 | 0.803 | 0.229 | 371 | 364.01 |
| 3DGS + Low Degree SH | 27.206 | 0.812 | 0.219 | 341 | 517.45 |
| 3DGS + Multi-Axis Orthogonal SG + Mix SH (Ours) | 27.267 | 0.813 | 0.218 | 334 | 416.02 |

Table 2: Ablation studies on the Mip-NeRF360 dataset.

| Dataset | Mip-NeRF360 | Tanks&Temples | DeepBlending |
|-----------------------|-------------|---------------|--------------|
| 3D Gaussian Splatting | 781.46 | 434.10 | 662.26 |
| SG-Splatting | 416.02 | 228.78 | 357.45 |

Table 3: Comparison of storage size (in MB) for 3D Gaussian Splatting and SG-Splatting.

The orthogonal arrangement of the SGs still captures the details of the scene effectively, enabling faster rendering and better storage efficiency.

3DGS + Low Degree SH: To rigorously evaluate the effectiveness of spherical Gaussians (SG), we also conducted ex-

periments using low-degree spherical harmonics (SH). This setup simplifies the representation, achieving a moderate improvement in rendering speed (341 FPS compared to the original 247 FPS) and a reduction in model size to 517.45 MB.

3DGS + Multi-Axis Orthogonal SG + Mix SH (Ours): In this configuration, we combine the advantages of low-degree spherical harmonics (SH) and spherical Gaussians (SG) to achieve a balanced trade-off between rendering quality, speed, and model size. Compared to the original 3D-GS, our method maintains comparable rendering quality (PSNR: 27.267 vs. 27.410, SSIM: 0.813 vs. 0.814) while significantly improving efficiency. Specifically, our method achieves a higher rendering speed (334 FPS compared to 247 FPS) and a notably smaller model size (416.02 MB compared to 781.46 MB). Using the complementary strengths of SG and low-degree SH, this approach provides an effective solution for scenarios requiring both high-performance and compact model storage.

Conclusion

In this paper, we propose SG-Splatting, a 3D Gaussian Splatting technique designed to address the limitations of 3D Gaussian Splatting, especially the excessive number of third-degree spherical harmonic coefficients that hinders rendering speed. Our approach utilizes Spherical Gaussians for a more compact color representation, to mitigate the issues of coefficient overload and slow inference times. Additionally, we incorporate multiple Spherical Gaussians and mix them with adaptive low-degree spherical harmonics to enhance rendering quality while maintaining fast rendering speeds. Moreover, SG-Splatting is designed to be plug-and-play, allowing it to be easily integrated into other acceleration techniques without compromising performance.

References

- Barron, J. T.; Mildenhall, B.; Verbin, D.; Srinivasan, P. P.; and Hedman, P. 2022. Mip-NeRF 360: Unbounded Anti-Aliased Neural Radiance Fields. In *Proceedings of the IEEE/CVF Conference on Computer Vision and Pattern Recognition (CVPR)*, 5470–5479.
- Fan, Z.; Wang, K.; Wen, K.; Zhu, Z.; Xu, D.; and Wang, Z. 2023. LightGaussian: Unbounded 3D Gaussian Compression with 15x Reduction and 200+ FPS. *arXiv:2311.17245*.
- Fang, G.; and Wang, B. 2024. Mini-Splatting: Representing Scenes with a Constrained Number of Gaussians. *arXiv preprint arXiv:2403.14166*.
- Girish, S.; Gupta, K.; and Shrivastava, A. 2023. Eagles: Efficient accelerated 3d gaussians with lightweight encodings. *arXiv preprint arXiv:2312.04564*.
- Hamdi, A.; Melas-Kyriazi, L.; Mai, J.; Qian, G.; Liu, R.; Vondrick, C.; Ghanem, B.; and Vedaldi, A. 2024. GES: Generalized Exponential Splatting for Efficient Radiance Field Rendering. In *Proceedings of the IEEE/CVF Conference on Computer Vision and Pattern Recognition (CVPR)*, 19812–19822.
- Hedman, P.; Philip, J.; Price, T.; Frahm, J.-M.; Drettakis, G.; and Brostow, G. 2018. Deep Blending for Free-viewpoint Image-based Rendering. *ACM Transactions on Graphics (Proc. SIGGRAPH Asia)*, 37(6): 257:1–257:15.
- Hedman, P.; Srinivasan, P. P.; Mildenhall, B.; Barron, J. T.; and Debevec, P. 2021. Baking Neural Radiance Fields for Real-Time View Synthesis. *ICCV*.
- Hinton, G.; Vinyals, O.; and Dean, J. 2015. Distilling the knowledge in a neural network. *arXiv preprint arXiv:1503.02531*.
- Jacob, B.; Kligys, S.; Chen, B.; Zhu, M.; Tang, M.; Howard, A.; Adam, H.; and Kalenichenko, D. 2018. Quantization and training of neural networks for efficient integer-arithmetic-only inference. In *Proceedings of the IEEE Conference on Computer Vision and Pattern Recognition (CVPR)*, 2704–2713.
- Jiang, Y.; Yu, C.; Xie, T.; Li, X.; Feng, Y.; Wang, H.; Li, M.; Lau, H.; Gao, F.; Yang, Y.; and Jiang, C. 2024. VR-GS: A Physical Dynamics-Aware Interactive Gaussian Splatting System in Virtual Reality. *arXiv preprint arXiv:2401.16663*.
- Kerbl, B.; Kopanas, G.; Leimkühler, T.; and Drettakis, G. 2023. 3D Gaussian Splatting for Real-Time Radiance Field Rendering. *ACM Transactions on Graphics*, 42(4): 139:1–139:14.
- Knapitsch, A.; Park, J.; Zhou, Q.-Y.; and Koltun, V. 2017. Tanks and Temples: Benchmarking Large-Scale Scene Reconstruction. *ACM Transactions on Graphics*, 36(4): 78:1–78:13.
- Mildenhall, B.; Srinivasan, P. P.; Tancik, M.; Barron, J. T.; Ramamoorthi, R.; and Ng, R. 2020. NeRF: Representing Scenes as Neural Radiance Fields for View Synthesis. In *European Conference on Computer Vision*, 405–421.
- Müller, T.; Evans, A.; Schied, C.; and Keller, A. 2022. Instant Neural Graphics Primitives with a Multiresolution Hash Encoding. *ACM Trans. Graph.*, 41(4): 102:1–102:15.
- Navaneet, K.; Meibodi, K. P.; Koohpayegani, S. A.; and Pirsavash, H. 2023. Compact3D: Compressing Gaussian Splat Radiance Field Models with Vector Quantization. *arXiv preprint arXiv:2311.18159*.
- Ng, R.; Ramamoorthi, R.; and Hanrahan, P. 2003. All-frequency shadows using non-linear wavelet lighting approximation. *ACM Trans. Graph.*, 22(3): 376–381.
- Niedermayr, S.; Stumpfegger, J.; and Westermann, R. 2023. Compressed 3D Gaussian Splatting for Accelerated Novel View Synthesis. *arXiv:2401.02436*.
- Schönberger, J. L.; and Frahm, J.-M. 2016. Structure-from-Motion Revisited. In *Proceedings of the IEEE Conference on Computer Vision and Pattern Recognition (CVPR)*, 4104–4113.
- Schönberger, J. L.; Zheng, E.; Pollefeys, M.; and Frahm, J.-M. 2016. Pixelwise View Selection for Unstructured Multi-View Stereo. In *European Conference on Computer Vision (ECCV)*.
- Shao, R.; Sun, J.; Peng, C.; Zheng, Z.; Zhou, B.; Zhang, H.; and Liu, Y. 2024. Control4D: Efficient 4D Portrait Editing with Text. In *Proceedings of the IEEE Conference on Computer Vision and Pattern Recognition (CVPR)*.
- Wang, J.; Ren, P.; Gong, M.; Snyder, J.; and Guo, B. 2009. All-frequency rendering of dynamic, spatially-varying reflectance. *ACM Trans. Graph.*, 28(5): 1–10.
- Wang, Z.; Bovik, A.; Sheikh, H.; and Simoncelli, E. 2004. Image quality assessment: from error visibility to structural similarity. *IEEE Transactions on Image Processing*, 13(4): 600–612.
- Xie, T.; Zong, Z.; Qiu, Y.; Li, X.; Feng, Y.; Yang, Y.; and Jiang, C. 2023. PhysGaussian: Physics-Integrated 3D Gaussians for Generative Dynamics. *arXiv preprint arXiv:2311.12198*.
- Xu, K.; Sun, W.-L.; Dong, Z.; Zhao, D.-Y.; Wu, R.-D.; and Hu, S.-M. 2013. Anisotropic Spherical Gaussians. *ACM Transactions on Graphics*, 32(6): 209:1–209:11.
- Yang, Z.; Yang, H.; Pan, Z.; and Zhang, L. 2024. Real-time Photorealistic Dynamic Scene Representation and Rendering with 4D Gaussian Splatting. In *International Conference on Learning Representations (ICLR)*.

Yu, A.; Li, R.; Tancik, M.; Li, H.; Ng, R.; and Kanazawa, A. 2021. PlenOctrees for Real-time Rendering of Neural Radiance Fields. In *Proceedings of the IEEE/CVF International Conference on Computer Vision (ICCV)*, 5752–5761.

Zhang, R.; Isola, P.; Efros, A. A.; Shechtman, E.; and Wang, O. 2018. The Unreasonable Effectiveness of Deep Features as a Perceptual Metric. In *Proceedings of the IEEE Conference on Computer Vision and Pattern Recognition (CVPR)*, 586–595.

Zhong, L.; Yu, H.-X.; Wu, J.; and Li, Y. 2024. Reconstruction and Simulation of Elastic Objects with Spring-Mass 3D Gaussians. *European Conference on Computer Vision (ECCV)*.

Zhou, X.; Lin, Z.; Shan, X.; Wang, Y.; Sun, D.; and Yang, M.-H. 2024. DrivingGaussian: Composite Gaussian Splatting for Surrounding Dynamic Autonomous Driving Scenes. In *Proceedings of the IEEE/CVF Conference on Computer Vision and Pattern Recognition (CVPR)*, 21634–21643.

Zwicker, M.; Pfister, H.; van Baar, J.; and Gross, M. 2002. EWA Splatting. *IEEE Transactions on Visualization and Computer Graphics*, 8(3): 223–238.

Reproducibility Checklist

1. This paper:

- Includes a conceptual outline and/or pseudocode description of AI methods introduced (yes)
- Clearly delineates statements that are opinions, hypothesis, and speculation from objective facts and results (yes)
- Provides well marked pedagogical references for less-familiale readers to gain background necessary to replicate the paper (yes)

2. Does this paper make theoretical contributions? (yes)

If yes, please complete the list below.

- All assumptions and restrictions are stated clearly and formally. (yes)
- All novel claims are stated formally. (yes)
- Proofs of all novel claims are included. (yes)
- Proof sketches or intuitions are given for complex and/or novel results. (yes)
- Appropriate citations to theoretical tools used are given. (yes)
- All theoretical claims are demonstrated empirically to hold. (yes)
- All experimental code used to eliminate or disprove claims is included. (yes)

3. Does this paper rely on one or more datasets? (yes)

If yes, please complete the list below.

- A motivation is given for why the experiments are conducted on the selected datasets. (yes)
- All novel datasets introduced in this paper are included in a data appendix. (NA)

- All novel datasets introduced in this paper will be made publicly available upon publication of the paper with a license that allows free usage for research purposes. (NA)

- All datasets drawn from the existing literature (potentially including authors' own previously published work) are accompanied by appropriate citations. (yes)

- All datasets drawn from the existing literature (potentially including authors' own previously published work) are publicly available. (yes)

- All datasets that are not publicly available are described in detail, with explanation why publicly available alternatives are not scientifically satisfying. (NA)

4. Does this paper include computational experiments? (yes)

If yes, please complete the list below.

- Any code required for pre-processing data is included in the appendix. (yes)

- All source code required for conducting and analyzing the experiments is included in a code appendix. (yes)

- All source code required for conducting and analyzing the experiments will be made publicly available upon publication of the paper with a license that allows free usage for research purposes. (yes)

- All source code implementing new methods have comments detailing the implementation, with references to the paper where each step comes from. (yes)

- If an algorithm depends on randomness, then the method used for setting seeds is described in a way sufficient to allow replication of results. (NA)

- This paper specifies the computing infrastructure used for running experiments (hardware and software), including GPU/CPU models; amount of memory; operating system; names and versions of relevant software libraries and frameworks. (partial)

- This paper states the number of algorithm runs used to compute each reported result. (yes)

- Analysis of experiments goes beyond single-dimensional summaries of performance (e.g., average; median) to include measures of variation, confidence, or other distributional information. (no)

- The significance of any improvement or decrease in performance is judged using appropriate statistical tests (e.g., Wilcoxon signed-rank). (no)

- This paper lists all final (hyper-)parameters used for each model/algorithm in the paper's experiments. (yes)

- This paper states the number and range of values tried per (hyper-) parameter during development of the paper, along with the criterion used for selecting the final parameter setting. (partial)